IEEE Access
Multidisciplinary | Rapid Review | Open Access Journal

Received August 18, 2019, accepted August 25, 2019, date of publication August 28, 2019, date of current version September 18, 2019.

Digital Object Identifier 10.1109/ACCESS.2019.2937993

Data-Driven Digital Direct Position Servo Control by Neural Network With Implicit Optimal Control Law Learned From Discrete Optimal Position Tracking Data

BAOCHAO WANG, (Member, IEEE), CHENG LIU, SAINAN CHEN, SHILI DONG, AND JIANHUI HU

School of Electrical Engineering and Automation, Harbin Institute of Technology, Harbin, China

Corresponding authors: Baochao Wang (baochao.wang@hit.edu.cn) and Jianhui Hu (hujianhui@hit.edu.cn)

ABSTRACT To get better control performance in motor control, more and more researches tend to apply non-linear control laws in the field of motor control. However, most conventional non-linear control theory is based on explicit model of controlled object and often resulting in complexity. Besides, the control parameters tuning is mainly aiming at stability of the system. No valid direct performance-oriented non-linear control theory has been proposed. Facing the limitations, this paper presents a direct motor position control in an implicit data-driven manner. Unlike conventional non-linear motor controls that are based on explicit models and with stability-based parameters tuning, this study gives performance-oriented non-linear control by mastering non-linear discrete optimal control law in an implicit data-learning manner. Firstly, optimal data of position tracking problem is obtained by solving optimization problem. Secondly, the implicit discrete optimal control law hidden in data is learned by a BP neural network. Finally, the learned control law is implemented in real-time control to reproduce optimal control performance. Simulation and experiment results validated the feasibility of the data-driven controller, which could be helpful for performance-oriented non-linear control designs. The merits and further improvements are also discussed.

INDEX TERMS Position control, implicit discrete optimal control, artificial neural network, motor, data learning.

I. INTRODUCTION

Conventional motor control designs are based on explicit models or relations. For example, the commonly used PID three-loop position control structure in engineering is based on frequency domain model. For other complex control strategies, such as adaptive control, recursive control, back-stepping control, sliding mode control, H-infinity control, model reference control, etc. [1]–[8], the explicit model-based analysis is also indispensable. It is often supposed that non-linear control is able to achieve better performance than linear control. However, the non-linear control designs are often based on Lyapunov stability theory that aims at stability or stability-oriented control parameter tuning, not directly oriented to performance. In recent years, model reference control has drawn a lot of attentions, and it is not dependent on Lyapunov theory, but the finite enumeration and relative optimum selection in model reference control make it quite computation-demanding. Facing the bottlenecks, the authors wonder if there is an absolute optimal non-linear control law, which can be implicitly expressed and mastered to get better position control performance.

Data-driven control is one kind of model-free control originating from computer science. It is designed only by the input and output data and has no relation with structural information [9]. Literature [10] gives a comprehensive description of model-free adaptive control (MFAC) including the theoretical analysis of the bounded-input bounded-output stability. Data-driven control can be used to tune controller parameters or to perform system identification, as well as to directly approximate the control signal itself [11]–[13]. Two common data-driven control methods in motor control field are the PID type control technique based on the classical PID control, and the applications of artificial neural network technique in adaptive

The associate editor coordinating the review of this article and approving it for publication was Sotirios Goudos.

control [14]. Also the data-driven control can be combined with other control methods. In [15], a data-driven active disturbance rejection control (ADRC) is combined with a proportional-derivative Takagi-Sugeno Fuzzy (PDTSF) logic controller. The control performance is validated in a tower crane system.

With the development of software and hardware in recent years, artificial neural network has regained attentions for significantly improving the performance of many intelligent processing tasks [16]–[24], such as image classification, speech recognition, object detection, face recognition, semantic separation, machine translation, pedestrian detection, video analysis, as well as the game of Go.

The main advantage of neural network is that it is able to approximate certain relationship without explicitly knowing it, i.e. it can learn some hidden laws from the given data. This kind of relations vary from how to drive a car to how to mimic a simple non-linear relation.

In the field of motion control, neural network is not as hot as in the other applications, and the existing implementations can be mainly classified into two groups: tuning controller gain or assisting controller output.

In the first group, neural network is used to tune controller gain. In [25], a wavelet fuzzy neural network is used for online parameter tuning of an integral-proportional speed controller used in maximum-torque-per-ampere vector control of an interior permanent magnet synchronous motor. The neural network increases or decreases the controller gain to get a faster response during dynamic transients. In [26], a fuzzy neural network is adopted to adjust the control gain of sliding mode controller to meet the sliding mode condition. In [27], a neural network is used to provide suitable gains for PI controller according to detected operating condition. In [28], a neural network is used to adjust the fuzzy controller output scaling factor to improve dynamic characteristics of a ultrasonic motor.

In the second group, neural network is used together with other main controller to compensate total output. In [29], a wavelet neural network is used in parallel to adjust the H∞ controller output, in order to compensate the uncertainty bound for H∞ control. In [30], B-Spline neural network is used to approximate a nonlinear term containing position reference and position error to improve main controller performance. In [31], recurrent-fuzzy-neural-network is combined with sliding mode controller for real-time adjustment of uncertainty boundaries. In [32], a wavelet neural network is used in parallel with a robust controller for rotor position control of an induction servo motor. In [33], fuzzy neural network is used with model reference control for position control of a ultrasonic motor.

Besides using neural network with controllers, other applications also include parameter estimation [34], fault diagnostics [35], etc.

To sum up, in the literatures, the neural network has not been directly used as a main controller for motor position servo control, nor is it used for pursuing optimal control performance. This paper explores the feasibility of directly using an artificial neural network to fully realize position control of a motor, while learning a discrete optimal control law that is difficult to achieve. The used motor in this study is a voice coil motor (VCM), which does not contain ferromagnetic materials in the armature, and the motive force is induced by conductors that carrying current in a magnetic field [36]. The motion type involves linear, rotary or planar. It is widely used in high-performance-demand servo applications such as semiconductor manufacturing, active vibration reduction, precision machining, etc. The neural network is used to learn a discrete optimal control law hidden in optimal position tracking data.

Getting optimal performance in practice is very attractive as it is the ''best'' performance with limited control resource in given conditions. Conventional theory of optimal control was established for continuous system. When applying continuous optimal control law in discrete/digital control, the chattering problem is unavoidable. Various improvements are performed, such as increasing sampling frequency, using more smooth saturation function instead of sign function, smoothing algorithm, combination with other controllers, piecewise linearization etc. [37]–[39]. However, these improvements are performed on continuous control law. They can alleviate chattering but not completely eliminate chattering. Fuzzy controller is another non-linear controller which is often used to get optimal performance. Literature [40] uses a fuzzy controller in a two degree-of freedom cross-coupling system and gets better control performance than LQR controller. In [41], fuzzy controller is applied together with model-free sliding mode in optimization problem. Literature [42] develops an adaptive iterative learning reliable control (AILRC) strategy which can compensate input saturation and state delays without need for precise system parameters. Some other intelligence control methods are also investigated such as particle swarm optimization [43].

It is pointed out by Prof. Han Jingqing that the continuous optimal control law (together with improvements on it) is not optimal for discrete/digital control. Continuous laws cannot reach the desired control reference with finite steps. However, this point has not drawn much attention in literatures. Prof. Han has proposed a discrete optimal control law for second order cascade integral plant, namely ''fhan'', which is successfully used in Active Disturbance Rejection Control (ADRC) [44]. ADRC algorithm has been successfully used in many applications and has also been packaged in microcontroller chips by Texas Instrument and Freescale. Future discussion on discrete optimal control law is provided in Section VI of this paper. A discrete optimal control law is more complicated than continuous optimal control law. Besides, when taking into account of damping factors (such as resistor, friction, viscosity), inner dynamic loops or high-order features, an analytical discrete optimal control law can be too difficult to obtain explicitly (also difficult for continuous case).

The optimal control law for motor position control is of high order, in discrete time and with damping factors. Thus, an analytical relation can hardly be obtained. Inspired by the progress of artificial intelligence applications, numerically obtaining the optimal control data and implicitly mastering the hidden discrete optimal control law by a neural network are proposed in this paper.

The rest of this paper is organized as follows: Section II introduces the VCM model and the acquisition of optimal position tracking data through optimization problem solving. Neural network principles and its training with the obtained optimal position tracking data are given in Section III. Simulation and experiment results are given in Section IV and Section V respectively. Discussions on control performance and practical issue are provided in Section VI. Section VII concludes this paper.

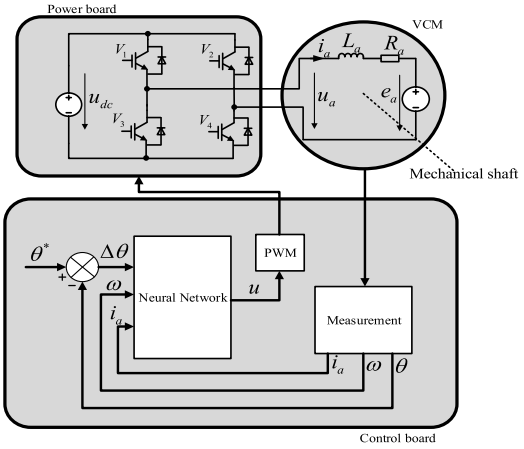

FIGURE 1. Overview of the proposed control algorithm.

II. PLANT DESCRIPTION AND OPTIMAL DATA ACQUISITION

The proposed direct position control structure overview is given in FIGURE. 1. Given the position tracking error, angular velocity and current, the trained artificial neural network gives the output voltage u to drive the VCM. A Rotary VCM (RVCM) is used for implementation in this paper.

Data is essential for neural network learning. In this study, the optimal control position tracking data of various circumstances is obtained by numerically solving an optimization problem. The required plant model and the optimization problem are given in this section.

A. MATHEMATICAL MODEL OF THE RVCM

The block diagram of RVCM is shown in FIGURE. 2 and the state space model is presented in (1).

$$\begin{cases} \dfrac{d\theta}{dt} = \omega \\ \dfrac{d\omega}{dt} = \dfrac{k_t}{J} i_a - \dfrac{k}{J}\omega - \dfrac{1}{J} T_l \\ \dfrac{di_a}{dt} = \dfrac{1}{L_a} u_a - \dfrac{k_e}{L_a}\omega - \dfrac{R_a}{L_a} i_a \end{cases} \tag{1}$$

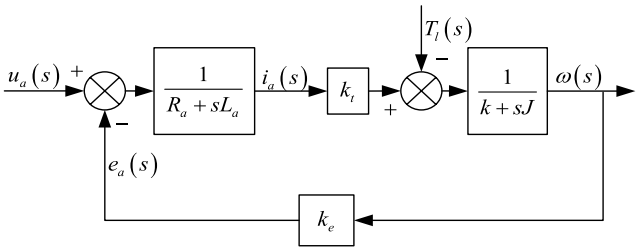

FIGURE 2. Block diagram of RVCM.

where θ is the position of the mover (rad); ω is the angular velocity (rad/s); u_a, i_a, R_a and L_a are respectively terminal voltage (V), current (A), resistance (Ω) and the inductance (H) of the VCM armature; e_a is the Back Electromotive Force (BEMF, V); k_a is BEMF coefficient (V·s/rad); T_e is the electromagnetic torque (Nm); T_l is the load torque (Nm); k_t is the torque coefficient (Nm/A); j is the inertia of the moving part (kg·m^2); k is the viscosity damping coefficient (Nm·s/rad). The main parameters of RVCM are presented in TABLE 1.

TABLE 1. Main parameter of the RVCM.

Symbol	Description	Value	Unit
R_a	Armature resistance	4.41	Ω
L_a	Armature inductance	1.87	mH
k_t	Torque coefficient	0.3	Nm/A
k_e	BEF coefficient	0.3	V·s/rad
J	Rotational inertia	0.00012	kg·m^2
k	Viscosity damping coefficient	0.0233	Nm·s/rad
V_{dc}	Driving voltage	7	V

B. OPTIMIZATION PROBLEM FORMATION AND SOLUTION

Optimal position tracking data is obtained by solving an optimization problem. The optimization formulation must consider both optimization objective and constraints.

The optimization objective is that the RVCM position x_1 can be controlled to follow the given position reference x_1^*. The objective is mathematically expressed by minimizing the sum of squared error of position tracking, as in (2).

$$\text{Minimize } obj = \sum_{i=1}^{m} \left(x_1[i] - x_1^*[i]\right)^2 \tag{2}$$

where obj is the objective value to be minimized in optimization, whose value is used to express the position control tracking quality; i is the discrete step index; m is the maximum discrete step index.

Regarding constraints, the motor model should be firstly considered. In order to form the optimization problem with

less computations, the plant model in (1) is simplified as (3).

$$\begin{cases} \dot{x}_1 = x_2 \\ \dot{x}_2 = k_1 x_3 - k_2 x_2 - k_3 T_l \\ \dot{x}_3 = k_4 u_a - k_5 x_2 - k_6 x_3 \end{cases} \tag{3}$$

where

$$\begin{cases} x_1 = \theta, x_2 = \omega, x_3 = i_a \\ k_1 = \dfrac{k_t}{J}, k_2 = \dfrac{k}{J}, k_3 = \dfrac{1}{J}, k_4 = \dfrac{1}{L_a}, k_5 = \dfrac{k_e}{L_a}, k_6 = \dfrac{R_a}{L_a} \end{cases} \tag{4}$$

The discrete form of (3) is used as optimization problem constraints, as given in (5).

$$\begin{cases} x_1[i] = x_1[i-1] + h x_2[i-1] \\ x_2[i] = x_2[i-1] + h\left(k_1 x_3[i-1] - k_2 x_2[i-1]\right) \\ x_3[i] = x_3[i-1] \\ +h\left(k_3 u_a[i-1] - k_4 x_2[i-1] - k_5 x_3[i-1]\right) \end{cases} \tag{5}$$

where h is the discrete sampling time step size.

Another constraint is the inverter output voltage. The H-bridge inverter PWM chopping output is limited by the DC voltage, expressed in (6).

$$-u_{DC} < u[i] < u_{DC} \tag{6}$$

To sum-up, the overall optimization problem formulation is given in (7), and the initial values of corresponding variables are set to zero.

$$\text{Minimize } obj = \sum_{i=1}^{m} \left(x_1[i] - x_1^*[i]\right)^2$$

$$\text{subject to } \begin{cases} x_1[i] = x_1[i-1] + h x_2[i-1] \\ x_2[i] = x_2[i-1] \\ +h\left(k_1 x_3[i-1] - k_2 x_2[i-1]\right) \\ x_3[i] = x_3[i-1] \\ +h\left(k_3 u_a[i-1] - k_4 x_2[i-1] - k_5 x_3[i-1]\right) \\ -u_{DC} \le u_a[i] \le u_{DC} \\ x_1[0] = 0 \\ x_2[0] = 0 \\ x_3[0] = 0 \\ u_a[0] = 0 \end{cases}$$

$$i = 1, 2, 3, \ldots \tag{7}$$

Given specific external conditions for the above formulation, i.e. the desired reference position trajectory x_1^* and load torque T_l, the optimal position tracking control sequence of u_a together with the evolutions of x_1, x_2 and x_3 can be obtained.

Noting that constraints in (7) eventually result in numerous equations according to different values taken by index i, the optimization problem size is huge. The optimization problem is formulated with C++ programming language and is solved by a specific optimization solver.

C. OPTIMIZATION RESULT

After solving the optimization problem, the optimal position tracking data is obtained, including θ, ω, i_a, u_a. The corresponding discrete sampling frequency is set to 5 KHz. The obtained optimal position tracking results for different step size within 0.1∼0.3 rad are shown in FIGURE. 3.

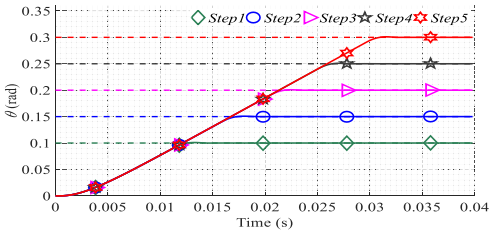

FIGURE 3. Optimization results for different position tracking step size.

From the optimal position tracking results in FIGURE. 3, it can be seen that the settling times is almost proportional to the stepping size, which may be considered as granted. However, when using error-driven PID controller, the relation between settling time and stepping size could be different, which is further discussed in Section VI.

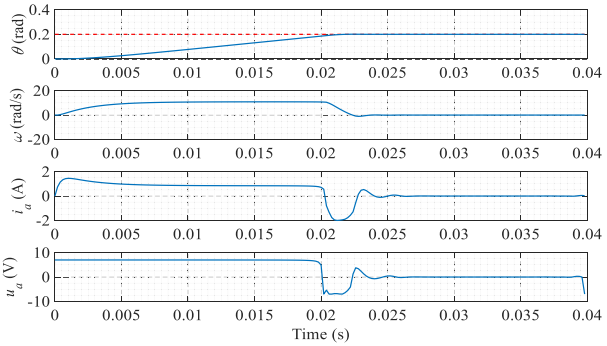

FIGURE 4. Detailed optimization results for position tracking of 0.2rad stepping.

FIGURE. 4 demonstrates a detailed evolution of all status variables in one case of the optimal position tracking. It can be seen that the optimal position tracking process includes different phases of acceleration (0s∼0.005s), constant velocity (0.005s∼0.02s), deceleration (0.02s∼0.0225s), stabilization (0.0225∼0.0265s). The stabilization phase is also very important to reach steady state position with finite discrete steps without oscillation. During the acceleration, constant speed and deceleration process, it can be seen the limited 7V control voltage is fully used, which shortens the response time and makes the optimal relation quite non-linear.

III. NEURAL NETWORK PRINCIPLE AND ITS TRAINING WITH OBTAINED OPTIMAL POSITION TRACKING DATA

The optimization results implicitly describe the optimal control law in the given conditions. Neural network is trained by the obtained data to learn such optimal control law.

The objective is to reproduce such optimal relation in real-time control. In this paper, Back Propagation (BP) neural network is chosen for position servo control of RVCM.

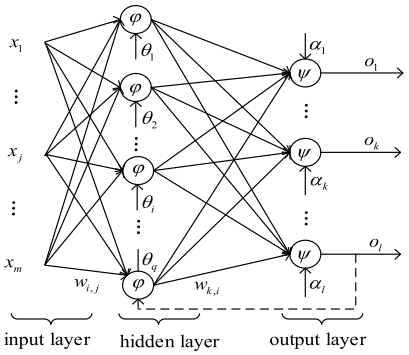

FIGURE 5. The structure of feedforward neural network.

A. BRIEF INTRODUCTION OF BP NEURAL NETWORK

BP neural network is a feedforward neural network with back propagation (BP) learning algorithm. A basic structure is given in FIGURE. 5. The network consists of input layer, hidden layer, and output layer. Multiple hidden layers can also be used.

Input layer specifies the input of the network. Hidden layer and output layer process their corresponding input by artificial neurons.

Each neuron performs a non-linear calculation with parameters of weight and threshold. Take the i^{th} neuron in hidden layer for example, the corresponding weight and threshold are noted as w_{ij} and θ_i. As shown in the figure, j is input variable index ($j = 1, 2, \ldots, m$), and i is the neuron index ($i = 1, 2, \ldots q$). The i^{th} neuron calculation can be expressed by (8) and (9).

$$net_i = \sum_{j=1}^{m} w_{ij}x_j + \theta_i \tag{8}$$

where net_i is linear part of the neuron calculation, and the non-linear feature of the neuron is expressed by (9).

$$y_i = \varphi\left(net_i\right) = \varphi\left(\sum_{j=1}^{m} w_{ij}x_j + \theta_i\right) \tag{9}$$

where y_i is the output of the i^{th} neuron, and φ is a non-linear function called excitation function. The often used excitation functions include S-shaped tangent function (tansig), S-shaped logarithmic function (logsig), and a pure linear function (purelin) as shown in FIGURE. 6.

The output layer performs similar neuron calculations, and finally k^{th} output o_k in this example can be expressed as:

$$o_k = \psi\left(net_k\right) = \psi\left[\sum_{i=1}^{q} w_{ki}\varphi\left(\sum_{j=1}^{m} w_{ij}x_j + \theta_i\right) + a_k\right] \tag{10}$$

where w_{ki} and a_k are respectively weight and threshold of neuron k in the output layer, and ψ is the excitation function.

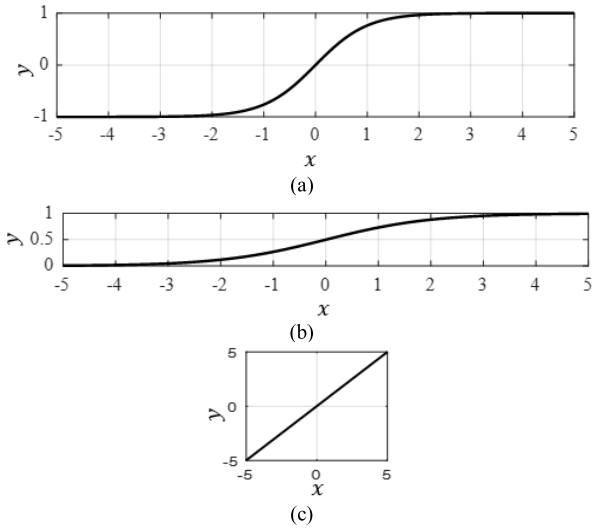

FIGURE 6. Different excitation functions of a neuron. (a) Transig; (b) Logsig; (c) Purelin.

B. NEURAL NETWORK CONFIGURATION AND TRAINING

In this study, the used BP network parameters are given in Table 2.

TABLE 2. Neural network parameters.

Name	Value
Input variables	$\Delta\theta, \omega, i_a$
Target variables	u_a
Number of layers for Hidden layer	2
Number of neurons in Hidden layer	12
Excitation function type	tansig

The selection of the number of neurons in hidden layer is a difficult point in the design of BP neural network. No specific formula has been drawn, and it can only be tested specifically for specific problems. After comparing the training effects of different neuron numbers, the number of neurons in hidden layer is selected as 12. In the configured network, the corresponding weights and thresholds have to be adjusted by data training using the obtained optimal data in Section II.

The data learning/training is where the so-called "back propagation" plays its role. When the network output does not match the training data, the error is returned to modify the weights and thresholds of the network so that the error gradient decreases. It is equivalent as solving an optimization problem. The training can be easily performed with software tools such as MATLAB. After training with the optimal data, the Neural Network is ready to use for position control.

IV. SIMULATION

After being trained by the optimal position tracking data obtained for stepping response, so far, we have already got the neural network controller. In this section, the neural network

will be put in the control scheme just like FIGURE 1, and will be validated. The neural network is firstly tested for simulation in MATLAB/Simulink. The model and parameters of the voice coil motor we used shown in FIGURE 2 and TABLE 1. The control frequency is set to 5kHz, which is the same as optimization model step size. Different cases using in-training and out-of-training conditions are tested. The in-training condition refers to the cases that performed with optimization and whose data is used for training neural network. The out-of-training condition refers to the cases that are not included in optimization and training.

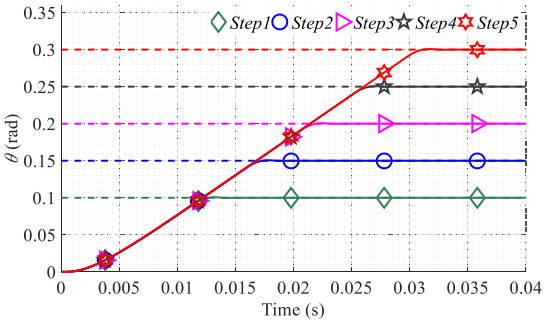

FIGURE 7. Simulation results for in-training position tracking with different position stepping size.

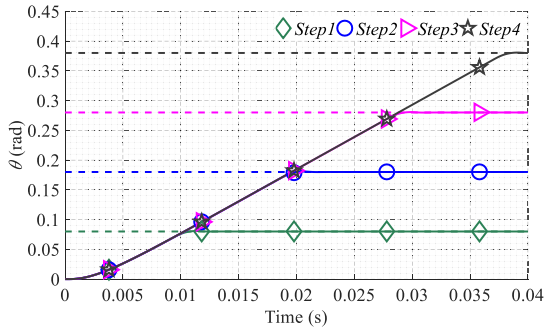

FIGURE 8. Simulation results for out-of-training position tracking with different step size.

Firstly, five in-training cases with different step size are tested. FIGURE. 7 shows the position tracking performance for in-training condition. By comparing with the optimization results in FIGURE. 3, it can be seen that the simulated results are almost the same as optimization. Thus, the artificial neural network can not only learn hidden relation from the optimal data, but also reproduce such optimal control strategy for instantaneous control.

Secondly, four out-of-training cases are also performed. It can be seen that the responses are fast and without overshoot. The responses are consistent with in-training data. It is validated that by only a part of data learning, the neural network is able to master the hidden control law, which is general to certain degree, so that it can be used for other unlearned data.

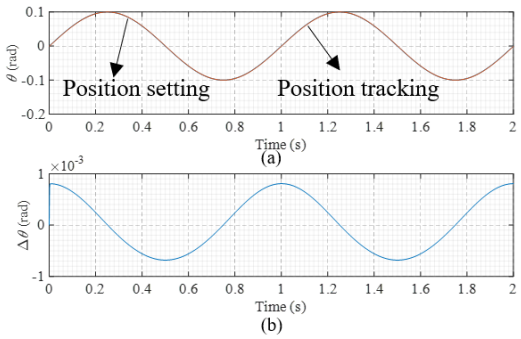

FIGURE 9. Simulation results for out-of-training sinusoidal position tracking.

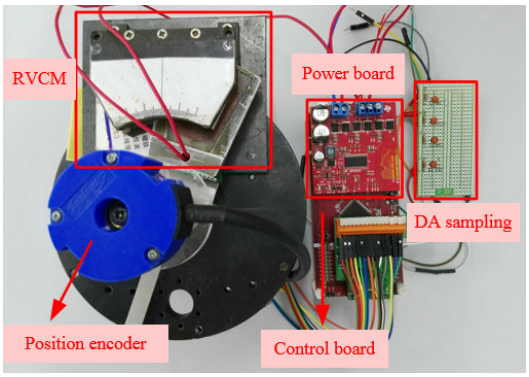

FIGURE 10. Experiment rig.

Finally, to further validate the feasibility and adaptive of the control. A out-of-training case of sinusoidal tracking is also performed. The obtained results of position tracking waveform and corresponding error are given in FIGURE. 9. The position is able to track the reference. The maximum error is less than 0.0008rad, which occurs during the position tracking zero-crossing instant. The maximum error is less than 1% of the peak position tracking amplitude. Thus, the feasibility of data-trained artificial network is further validated. It is also proved that the proposed control strategy does not need to learn all cases of position tracking, learning part of the cases can master the general control law.

V. EXPERIMENTAL TESTS

According to the controller design in Section II and Section III and the simulation results of Section IV, experimental tests are carried out to evaluate the proposed data-driven artificial neural network position control. During experiment conditions, the non-ideal measurement, inverter nonlinearity (such as PWM dead-time, voltage drop), model uncertainty, etc. could have negative influence on the control performance.

The experiment rig is shown in FIGURE. 10. The artificial neural network is implemented with TI TMS320F28377S controller. The algorithm execution time is 84μs in the 200MHz DSP. The code for the control algorithm is written in C and compiled in the TI CCS environment. FPGA implementation is also attractive for its great potential in

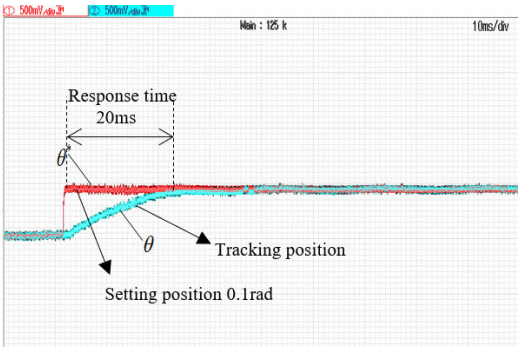

FIGURE 11. Experiment result for 0.1rad step size.

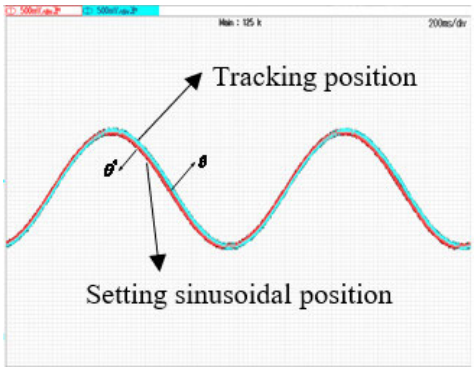

FIGURE 13. Experiment result for sinusoidal position tracking.

neural network parallel computation. The encoder resolution is 0.00628 rad. The position tracking signals are transformed from controller data through a digital-to-analog circuit using a 1MHz High Resolution PWM with a low-pass RC filter.

FIGURE. 11 gives the performance of 0.1rad step size. It can be seen that the response is smooth and without overshoot. The position tracking settling time is about 20ms, which is longer than 11ms in the ideal case of simulation and optimization. As aforementioned, during experiment, various factors such as the model uncertainty, dead band, velocity calculation, measurement resolution, noise and filtering could affect the experimental results. This slower response is identified mainly caused by velocity calculation, which is further discussed in the following section. Even with these factors, the control performance is stable.

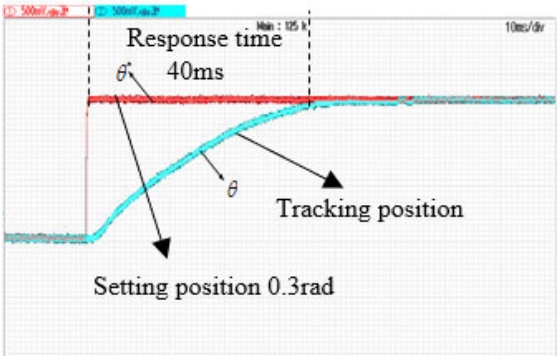

FIGURE 12. Experiment result for 0.3rad step size.

FIGURE. 12 gives the position tracking performance of 0.3rad step. The position tracking is also smooth and without overshoot. The position settling time is about 40ms.

FIGURE. 13 gives a position tracking performance for sinusoidal position tracking. The tracking position waveform is quite sinusoidal, with a phase error about 2°. As aforementioned, the neural network is only trained with step response. The successful tracking of sinusoidal position demonstrates that although the artificial network is trained with a small amount of data, control-law therein is universal for other control situations. This result further validated the feasibility of using artificial neural network for direct position control.

VI. DISCUSSION

This section provides a further discussion on the proposed direct position control by artificial neural network through optimal data learning, including comparison with PID controller, the reason for slower response in experiment, as well as the comparison of continuous and discrete control law (or the reason to use neural network).

A. COMPARISON WITH PID CONTROLLER

The proposed artificial neural network control is based on the optimal data, in order to learn an optimal control law that is difficult to obtain analytically. For the optimal control, the larger the position step size, the longer the position tracking time. This response time relation with step size may be taken for granted. However, it is not the exactly the case for PID controller, which is discussed in detail as follows.

A PID controller can be configured to work in linear mode (the output always between minimum and maximum output limit, without saturation) or non-linear mode (the output may take the value of minimum and maximum limit, with saturation). In this application, the available control voltage is limited by DC bus voltage. In linear mode, the controller gain is selected as small value to ensure the output voltage does not exceed the limit. In non-linear mode, the controller is configured with an anti-windup/anti-saturation structure to make full use of limited control voltage.

For the PID controller in linear mode, the output is purely error driven. When the error is smaller, the output amplitude is low and the changing rate is slower. As a result, in this case one may observer that small step response takes much more time than large step, or the response time for tracking different reference is almost the same, as given by FIGURE. 14. As the error is small when approaching steady state, the response time takes about 1000ms.

In non-linear mode, the controller output is able to maintain the limit value during transients, and the limited output is more efficiently used. So the response time is smaller, as given by FIGURE. 15. Compared with linear mode,

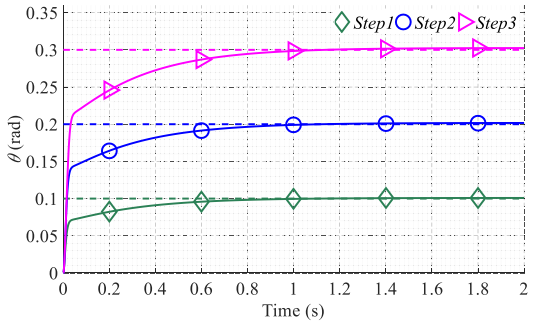

FIGURE 14. Position tracking with PID controller in linear mode.

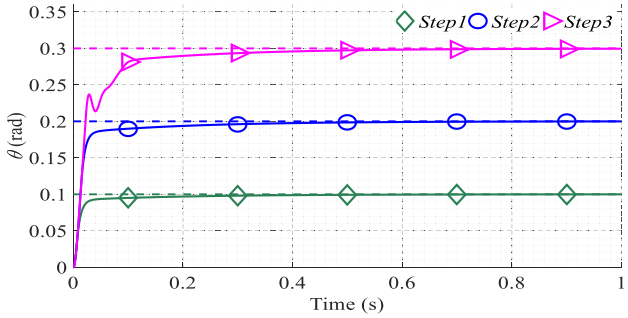

FIGURE 15. Position tracking with PID controller in non-linear mode.

the 95% settling time is reduced from about 550ms to 100ms. However, the saturation non-linearity is different for different references or stepping sizes. So it can be seen that for 0.3rad stepping (marked as step 3 in FIGURE. 15), the response transient is with overshoot and the response curve is not consistent with other response. For comparison, when using the proposed artificial neural network to learn optimal control law, the 95% settling time is less than 30ms.

B. VELOCITY CALCULATION INFLUENCE

The experimental settling time is slower than simulation, the main reason is identified as velocity calculation. During this control, the angular velocity is calculated through discrete encoder recorded position value. One recorded position trajectory data is shown in FIGURE. 16.

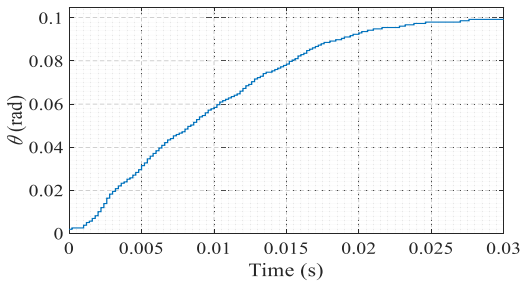

FIGURE 16. Recorded position tracking trajectory.

During the experiment test, the velocity is calculated by direct calculation. With the discrete time sampling and limited sensor resolution, the calculated velocity is not

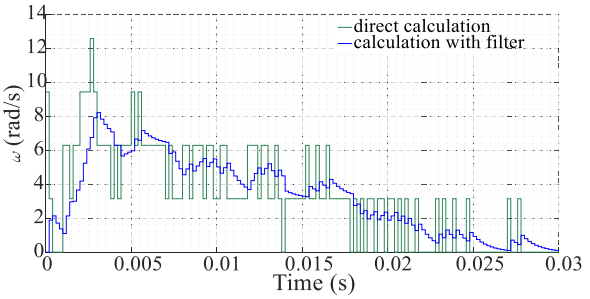

FIGURE 17. Calculated angular velocity.

smooth and with oscillations, as shown by the green curve in FIGURE. 17. This oscillation is not consistent as in the velocity in ideal case of optimization and simulation, such as the velocity shown in FIGURE. 4, which could affect the judgment of acceleration and deceleration of the optimal control law. Eventually this wrong judgment could slow the step response, which is the main reason of slower response in experimental tests. When implementing simple filtering, velocity measurement delay and transient amplitude reduction could also be an issue. Future work should be carried out to improve the velocity calculation.

Another effective yet direct way is to improve the position sensor resolution. If further analyzing the position trajectory in FIGURE. 16, it can be discovered that the position trajectory span includes 159 minimum position resolutions, and the whole time span includes 150 sampling. Thus, at adjacent sampling moments, the position increment is only 0, 1, 2, 3, or 4 times of minimum position resolution, which cause the velocity calculation oscillation as shown in FIGURE. 17. Increasing the position sensor resolution can efficiently solve this velocity calculation issue.

C. CONTINUOUS VS DISCRETE OPTIMAL CONTROL LAW

This paper gives the approximation to obtain high order discrete optimal control law by means of neural networks. Why the discrete optimal control law is difficult to obtain and the differences between continuous and discrete optimal control laws are discussed in this part.

For simplicity, we will try to clarify this problem with a second order cascade integral plant with limited control signal u ($|u| \leq r$), as expressed in (11).

If such a second order plant refers to a case of motor position control, x_1 can be considered as the position, x_2 is the velocity, the control signal u is a limited Force/Torque.

$$\begin{cases} \dot{x}_1 = x_2 \\ \dot{x}_2 = u, |u| \leq r \end{cases} \tag{11}$$

If position x_1 requires to converge to x_1^*, the velocity must satisfy $x_2 = 0$ at $x = x_1^*$. Conventional continuous optimal control law with minimum time can be obtained as:

$$u = -r\text{sign}(x_1 - x_1^* + \frac{x_2 |x_2|}{2r}) \tag{12}$$

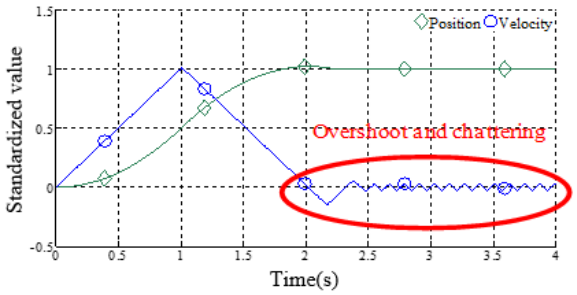

FIGURE 18. Continuous optimal control law performance in discrete control.

While implemented (12) in discrete/digital control case, it can result in overshoot and chattering, as given in FIGURE. 18.

The reason is identified by Prof. Han Jingqing as that discrete optimal control is completely different with the continuous optimal control law. The discrete optimal control law for the above system proposed by Prof. Han Jingqing is as follows [44]:

$$\begin{cases} d = rh^2, a_0 = hx_2, y = x_1 - x_1^* + a_0 \\ a_1 = \sqrt{d(d + 8\,|y|)} \\ a_2 = a_0 + sign(y)(a_1 - d)/2 \\ s_y = (sign(y + d) - sign(y - d))/2 \\ a = (a_0 + y - a_2)s_y + a_2 \\ s_a = (sign(a + d) - sign(a - d))/2 \\ fhan = -r(\dfrac{a}{d} - sign(a))s_a - rsign(a) \end{cases} \tag{13}$$

where h is the sampling time step.

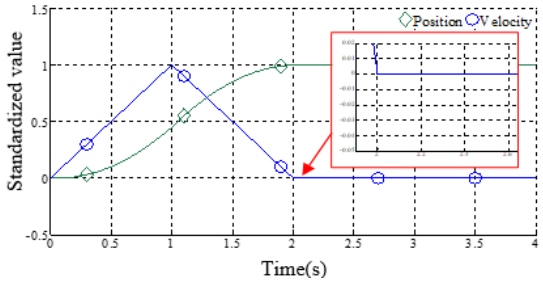

FIGURE 19. Discrete optimal control law performance in discrete control.

The control performance of (13) under the same condition is given in FIGURE. 19. This control law uses maximum accelerating and decelerating to achieve optimal control. It can be seen that the response is without overshoot or chattering, and the position settling transient time is shorter than that in FIGURE. 18.

As commented by Professor Han Jingqing, the continuous optimal control law (together with improvement on it) is not optimal for discrete control. They cannot reach the desired control reference with finite steps.

To sum up, it can be seen that the discrete optimal control law is different from the continuous optimal control law. The discrete optimal control law could be far more complicated than the continuous case.

Especially for a system of high order and complex internal dynamics, it is too difficult to get the explicit equation as "fhan" for second order cascade integral plant. That is why this paper studies the feasibility of approximating the discrete optimal control law through neural network data learning.

VII. CONCLUSION

This paper has proposed a data-driven digital direct position control method by neural network with implicit control law learned from optimal position tracking data. The contribution mainly includes: presenting a novel performance-oriented non-linear control design, demonstrating the feasibility of direct position control in a data-driven manner, implicitly mastering the discrete optimal control law that is difficult to obtain explicitly.

By learning several of optimal position tracking cases, the hidden general optimal control-law can be learned by the neural network and can be used for direct position control in real-time to reproduce an optimal control performance. The proposed method is validated by simulation and experimental results. In experiments, it is also found out that the velocity calculation has great influence on position tracking time. This issue can be improved by increasing position sensor resolution or improving velocity calculation.

Besides optimal position tracking data used in this study, using other types of data also provides potentials for other different control purpose, such as vibration reduction, harmonic suppression, etc. This technique also offers the possibility to learn from other controllers, or even combining the advantages of different controllers together. The data-driven study provides a point of view for performance-oriented non-linear control design in motor servo control.

REFERENCES

[1] E. Csencsics, M. Thier, R. Hainisch, and G. Schitter, "System and control design of a voice coil actuated mechanically decoupling two-body vibration isolation system," *IEEE/ASME Trans. Mechatronics*, vol. 23, no. 1, pp. 321–330, Feb. 2018.

[2] S.-Y. Chen and C.-Y. Lee, "Digital signal processor based intelligent fractional-order sliding-mode control for a linear voice coil actuator," *IET Control Theory Appl.*, vol. 11, no. 8, pp. 1282–1292, May 2017.

[3] J. Sun, G.-Z. Cao, S.-D. Huang, Y. Peng, J. He, and Q. Qian, "Sliding-mode-observer-based position estimation for sensorless control of the planar switched reluctance motor," *IEEE Access*, vol. 7, pp. 61034–61045, 2019.

[4] L. Su, Q. Hu, and L. Zhang, "Recursive decentralized control for trajectory tracking of flexible space manipulators," *IEEE Access*, vol. 7, pp. 39192–39206, 2019.

[5] B. Rui, Y. Yang, and W. Wei, "Nonlinear backstepping tracking control for a vehicular electronic throttle with input saturation and external disturbance," *IEEE Access*, vol. 6, pp. 10878–10885, 2017.

[6] M. G. López, P. Ponce, L. A. Soriano, A. Molina, and J. J. R. Rivas, "A novel fuzzy-PSO controller for increasing the lifetime in power electronics stage for brushless DC drives," *IEEE Access*, vol. 7, pp. 47841–47855, 2019.

[7] H. O. Erkol, "Optimal PI $^{\lambda}$ D $^{\mu}$ controller design for two wheeled inverted pendulum," *IEEE Access*, vol. 6, pp. 75709–75717, 2018.

[8] C.-M. Lin and H.-Y. Li, "A novel adaptive wavelet fuzzy cerebellar model articulation control system design for voice coil motors," *IEEE Trans. Ind. Electron*, vol. 59, no. 4, pp. 2024–2033, Apr. 2012.

[9] Y. Naung, A. Schagin, H. L. Oo, K. Z. Ye, and Z. M. Khaing, "Implementation of data driven control system of DC motor by using system identification process," in *Proc. IEEE Conf. Russian Young Res. Elect. Electron. Eng. (EIConRus)*, Jan./Feb. 2018, pp. 1801–1804.

[10] Z. Hou and S. Xiong, "On model free adaptive control and its stability analysis," *IEEE Trans. Autom. Control*, to be published.

[11] R. Cao, H. Zhou, H. Luo, and A. Su, "cSPACE-based data-driven control theory application for the linear servo system," in *Proc. 2nd Int. Conf. Mechanic Automat. Control Eng.*, Jul. 2011, pp. 130–133.

[12] R. Cao, H. Zhou, and Z. Hou, "The permanent magnet linear motor control based on data-driven control theory," in *Proc. Chin. Control Decis. Conf.*, May 2010, pp. 3164–3169.

[13] C. Rongmin, H. Zhongsheng, and H. Jian, "The model-free learning adaptive control for DC motor rotate speed systems," in *Proc. Chin. Control Conf.*, Jul. 2006, pp. 738–742.

[14] S. Khan, A. Paul, T. Sil, A. Basu, R. Tiwari, S. Mukherjee, U. Mondal, and A. Sengupta, "Position control of a DC motor system for tracking periodic reference inputs in a data driven paradigm," in *Proc. Int. Conf. Intell. Control Power Instrum. (ICICPI)*, Oct. 2016, pp. 17–21.

[15] R.-C. Roman, R.-E. Precup, E. M. Petriu, and F. Dragan, "Combination of data-driven active disturbance rejection and Takagi–Sugeno fuzzy control with experimental validation on tower crane systems," *Energies*, vol. 12, no. 8, p. 1548, Jan. 2019.

[16] D. Silver, J. Schrittwieser, K. Simonyan, I. Antonoglou, A. Huang, A. Guez, T. Hubert, L. Baker, M. Lai, A. Bolton, Y. Chen, T. Lillicrap, F. Hui, L. Sifre, G. van den Driessche, T. Graepel, and D. Hassabis, "Mastering the game of Go without human knowledge," *Nature*, vol. 550, no. 7676, pp. 354–359, Oct. 2017.

[17] D. Silver, A. Huang, C. J. Maddison, A. Guez, L. Sifre, G. van den Driessche, J. Schrittwieser, I. Antonoglou, V. Panneershelvam, M. Lanctot, S. Dieleman, D. Grewe, J. Nham, N. Kalchbrenner, I. Sutskever, T. Lillicrap, M. Leach, K. Kavukcuoglu, T. Graepel, and D. Hassabis, "Mastering the game of go with deep neural networks and tree search," *Nature*, vol. 529, no. 7587, p. 484–489, Jan. 2016.

[18] J. Schmidhuber, "Deep learning in neural networks: An overview," *Neural Netw.*, vol. 61, pp. 85–117, Jan. 2015.

[19] X. Zhang, L. Cheng, B. Li, and H.-M. Hu, "Too far to see? Not really!—Pedestrian detection with scale-aware localization policy," *IEEE Trans. Image Process.*, vol. 27, no. 8, pp. 3703–3715, Aug. 2018.

[20] K. Park, S. Kim, and K. Sohn, "Unified multi-spectral pedestrian detection based on probabilistic fusion networks," *Pattern Recognit.*, vol. 80, pp. 143–155, Aug. 2018.

[21] S. F. Dodge and L. J. Karam, "Visual saliency prediction using a mixture of deep neural networks," *IEEE Trans. Image Process.*, vol. 27, no. 8, pp. 4080–4090, Aug. 2018.

[22] X. Yuan, M. Sun, Z. Chen, J. Gao, and P. Li, "Semantic clustering-based deep hypergraph model for online reviews semantic classification in cyber-physical-social systems," *IEEE Access*, vol. 6, pp. 17942–17951, 2018.

[23] H. Li, H. Hu, and C. Yip, "Age-related factor guided joint task modeling convolutional neural network for cross-age face recognition," *IEEE Trans. Inf. Forensics Security*, vol. 13, no. 9, pp. 2383–2392, Sep. 2018.

[24] H. R. Roth, L. Lu, J. Liu, J. Yao, A. Seff, K. Cherry, L. Kim, and R. M. Summers, "Improving computer-aided detection using convolutional neural networks and random view aggregation," *IEEE Trans. Med. Imag.*, vol. 35, no. 5, pp. 1170–1181, May 2016.

[25] F.-J. Lin, Y.-T. Liu, and W.-A. Yu, "Power perturbation based MTPA with an online tuning speed controller for an IPMSM drive system," *IEEE Trans. Ind. Electron.*, vol. 65, no. 5, pp. 3677–3687, May 2018.

[26] F.-J. Lin and R.-J. Wai, "Sliding-mode-controlled slider-crank mechanism with fuzzy neural network," *IEEE Trans. Ind. Electron.*, vol. 48, no. 1, pp. 60–70, Feb. 2001.

[27] G.-J. Wang, C.-T. Fong, and K. J. Chang, "Neural-network-based self-tuning PI controller for precise motion control of PMAC motors," *IEEE Trans. Ind. Electron.*, vol. 48, no. 2, pp. 408–415, Apr. 2001.

[28] F.-J. Lin, R.-J. Wai, and S.-L. Wang, "A fuzzy neural network controller for parallel-resonant ultrasonic motor drive," *IEEE Trans. Ind. Electron.*, vol. 45, no. 6, pp. 928–937, Dec. 1998.

[29] F. F. M. El-Sousy, "Hybrid H-infinity-based wavelet-neural-network tracking control for permanent-magnet synchronous motor servo drives," *IEEE Trans. Ind. Electron.*, vol. 57, no. 9, pp. 3157–3166, Sep. 2010.

[30] C.-F. Hsu and Y.-C. Chen, "Microcontroller-based B-spline neural position control for voice coil motors," *IEEE Trans. Ind. Electron.*, vol. 62, no. 9, pp. 5644–5654, Sep. 2015.

[31] R.-J. Wai, "Total sliding-mode controller for PM synchronous servo motor drive using recurrent fuzzy neural network," *IEEE Trans. Ind. Electron.*, vol. 48, no. 5, pp. 926–944, Oct. 2001.

[32] R.-J. Wai, "Development of new training algorithms for neuro-wavelet systems on the robust control of induction servo motor drive," *IEEE Trans. Ind. Electron.*, vol. 49, no. 6, pp. 1323–1341, Dec. 2002.

[33] F.-J. Lin, R.-J. Wai, and R.-Y. Duan, "Fuzzy neural networks for identification and control of ultrasonic motor drive with LLCC resonant technique," *IEEE Trans. Ind. Electron.*, vol. 46, no. 5, pp. 999–1011, Oct. 1999.

[34] K. Liu and Z. Q. Zhu, "Position-offset-based parameter estimation using the adaline NN for condition monitoring of permanent-magnet synchronous machines," *IEEE Trans. Ind. Electron.*, vol. 62, no. 4, pp. 2372–2383, Apr. 2015.

[35] Y. Lei, F. Jia, J. Lin, S. Xing, and S. X. Ding, "An intelligent fault diagnosis method using unsupervised feature learning towards mechanical big data," *IEEE Trans. Ind. Electron.*, vol. 63, no. 5, pp. 3137–3147, May 2016.

[36] Y. Li, Y. Li, L. Ren, Z. Lin, Q. Wang, Y. Xu, and J. Zou, "Analysis and restraining of eddy current damping effects in rotary voice coil actuators," *IEEE Trans. Energy Convers.*, vol. 32, no. 1, pp. 309–317, Mar. 2017.

[37] D. Q. Zhang and G. X. Guo, "Discrete-time sliding mode proximate time optimal seek control of hard disk drives," *IEE Proc.-Control Theory Appl.*, vol. 147, no. 4, pp. 440–446, Jul. 2000.

[38] A. T. Salton, Z. Chen, and M. Fu, "Improved control design methods for proximate time-optimal servomechanisms," *IEEE/ASME Trans. Mechatronics*, vol. 17, no. 6, pp. 1049–1058, Dec. 2012.

[39] R. N. Danbury, "Near time-optimal control of nonlinear servomechanisms," *IEE Proceedings-Control Theory Appl.*, vol. 141, no. 3, pp. 145–153, May 1994.

[40] A. C. Soh, R. Z. A. Rahman, H. M. Sarkan, and L. T. Yeo, "Intelligent control of twin-rotor MIMO system using fuzzy inference techniques," *Int. Rev. Aerosp. Eng.*, vol. 6, no. 1, pp. 35–46, Jan. 2013.

[41] S. Vrkalovic, E.-C. Lunca, and I.-D. Borlea, "Model-free sliding mode and fuzzy controllers for reverse osmosis desalination plants," *Int. J. Artif. Intell.*, vol. 16, no. 2, pp. 208–222, 2018.

[42] H. Ji, Z. Hou, L. Fan, and F. L. Lewis, "Adaptive iterative learning reliable control for a class of non-linearly parameterised systems with unknown state delays and input saturation," *IET Control Theory Appl.*, vol. 10, no. 17, pp. 2160–2174, Nov. 2016.

[43] S. K. Goudos, K. B. Baltzis, C. Bahtsevanidis, and J. N. Sahalos, "Cell-to-switch assignment in cellular networks using barebones particle swarm optimization," *IEICE Electron. Express*, vol. 7, no. 4, pp. 254–260, 2010.

[44] J. Han, "From PID to active disturbance rejection control," *IEEE Trans. Ind. Electron.*, vol. 56, no. 3, pp. 900–906, Mar. 2009.

BAOCHAO WANG (S'10–M'14) was born in Jinan, China. He received the B.S. and M.S. degrees from the Harbin Institute of Technology (HIT), Harbin, China, in 2008 and 2010, respectively, and the Ph.D. degree from the University of Technology of Compiegne (UTC), Compiegne, France, in 2014, all in electrical engineering. Since 2014, he has been a Lecturer with the School of Electrical Engineering and Automation, HIT, where he is also with the State Key Laboratory of Robotics and System. His current research interests include PMSM drive and control, renewable energy integration, and power quality.

CHENG LIU was born in Tai'an, China. He received the B.S. degree in electrical engineering from the China University of Petroleum. He is currently pursuing the Ph.D. degree with the Laboratory of Microelectric Motor and Control, Harbin Institute of Technology, China. His research interests include motor control and electrical drives.

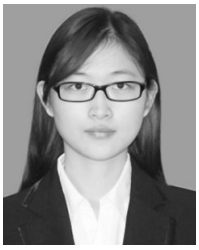

SAINAN CHEN was born in Jiangsu, China. She received the M.S. degree in electrical engineering from the Harbin Institute of Technology, in 2018. She is currently with the Midea Group, Guangdong. Her research interest includes advanced motion control and applications.

SHILI DONG was born in Yunnan, China. He received the B.S. and M.S. degrees in electrical engineering from the Harbin Institute of Technology, in 2016 and 2018, respectively. He is currently with Robotmeta, Shenzhen. His research interest includes the intelligent control of motors and robots.

JIANHUI HU was born in 1975. He received the B.S., M.S., and Ph.D. degrees from the Harbin Institute of Technology (HIT), Harbin, China, in 1998, 2000, and 2005, respectively, where he is currently an Associate Professor with the Department of Electrical Engineering. His research interests include variable flux permanent magnet motor and high torque density permanent magnet motor.